

Low Complexity Pre-Equalization Algorithms for Zero-Padded Block Transmission

Wenkun Wen, Minghua Xia, and Yik-Chung Wu

Abstract—The zero-padded block transmission with linear time-domain pre-equalizer is studied in this paper. A matched filter is exploited to guarantee the stability of the zero-forcing (ZF) and minimum mean square error (MMSE) pre-equalization. Then, in order to compute the pre-equalizers efficiently, an asymptotic decomposition is developed for the positive-definite Hermitian banded Toeplitz matrix. Compared to the direct matrix inverse methods or the Levinson-Durbin algorithm, the computational complexity of the proposed algorithm is significantly decreased and there is no bit error rate degradation when data block length is large.

Index Terms—Asymptotic equivalence, matched zero-padded (MZP) block transmission, pre-equalization.

I. INTRODUCTION

BLOCK transmission received a lot of attention in the past decade as it can remove the inter-block-interference (IBI) using simple measures and facilitate effective schemes for inter-symbol-interference (ISI) suppression [1]–[6]. Within the block transmission, the commonly used methods for IBI removal are the cyclic-prefix (CP) and zero-padding (ZP) schemes [7], [8]. Generally, the ZP scheme has higher power efficiency than the CP scheme, especially, when the channel has large delay spread such as underwater acoustic channel [9]. Moreover, the spectrum ripple of ZP scheme is much lower than that of CP scheme, since the correlation caused by the CP creates ripples into the average power spectral density of the transmitted signals. These features of ZP scheme make it attractive in power-limited systems [10], [11].

To combat ISI within each block of ZP block transmission, post-equalizer is usually exploited at the receiver side [8]. However, its inherent noise enhancement effect or error propagation will greatly reduce the output signal-to-noise ratio (SNR) and thus deteriorate system performance [12, Section 11.1]. On the other hand, if channel state information (CSI) is known at the transmitter, the transmitter can pre-equalize the transmitting signals by passing it through a filter that essentially pre-compensates the channel frequency response.

Compared to post-equalizer, one important feature of pre-equalizer is its capability to avoid the noise enhancement or error propagation. Furthermore, pre-equalization shifts the computational burden from the receiver to the transmitter.

Manuscript received March 19, 2009; revised February 10, 2010 and April 13, 2010; accepted May 31, 2010. The associate editor coordinating the review of this paper and approving it for publication was Y. Sanada.

W. Wen is with the New Postcom Equipment Co., Ltd., LTE R&D Center, Guangzhou 510663, China (e-mail: wenwenkun@newpostcom.com.cn).

M. Xia and Y.-C. Wu are with the Department of Electrical and Electronic Engineering, The University of Hong Kong, Pokfulam Road, Hong Kong (e-mail: {mhxia, ycwu}@eee.hku.hk).

Digital Object Identifier 10.1109/TWC.2010.061710.090411

Therefore, pre-equalizer is more appealing than post-equalizer in applications where simple receiver is desired.

In general, linear pre-equalizers such as zero forcing (ZF) and minimum mean square error (MMSE) schemes, are easy to be implemented due to low computational complexity. However, their performance is sensitive to the position of channel zeros [8], [13, Section 3.3.6]. There are two popular ways to deal with this problem. One is to add a modulus operation after the pre-equalizer such as in Tomlinson-Harashima precoder [14]–[16]. Another approach is to design a filter before pre-equalizer to guarantee its stability [17], [18].

In this paper, we take the latter approach. In particular, we investigate the stability of ZF and MMSE pre-equalizers and their low-complexity realization. First of all, a matched filter is designed to deal with the unstable channel inverse problem. Application of such matched filter before pre-equalizer results in the matched zero-padded (MZP) transmission. Then, an asymptotic decomposition on the positive-definite banded Toeplitz matrix is established, in order to compute the ZF and MMSE pre-equalizers efficiently. It is shown that the proposed algorithms incur no BER degradation when the data block length is large, but with a much lower computational complexity than the direct matrix inverse method or the Levinson-Durbin algorithm.

The rest of this paper is organized as follows. The signal model of block transmission is described in Section II. A matched filter for stable inverse of non-minimum phase channel is developed in Section III. Section IV establishes the asymptotic decomposition on the positive-definite Hermitian and banded Toeplitz matrix, and two fast pre-equalization algorithms are proposed. Simulation results are presented in Section V, and finally conclusions are drawn in Section VI.

For notational convenience throughout the paper, the operators $[\cdot]^*$, $[\cdot]^T$, $[\cdot]^H$, and $[\cdot]^{-1}$ denote the complex conjugate, transpose, Hermitian transpose, and inverse, respectively. The operator $\|\cdot\|_2$ refers to the \mathcal{L}_2 norm of a vector, and $\|\cdot\|_F$ stands for the Frobenius norm of a matrix. The operator $\|\mathbf{X}\|_w$ stands for the weak norm of \mathbf{X} defined as $\|\mathbf{X}\|_w = \sqrt{\frac{1}{N} \sum_{i=1}^N \sum_{j=1}^N |x_{ij}|^2}$, in which \mathbf{X} is a $N \times N$ complex matrix and x_{ij} is its $(i, j)^{\text{th}}$ entry. The operator $\|\mathbf{X}\|_s$ stands for the strong norm of \mathbf{X} defined as $\|\mathbf{X}\|_s = \max_{\mathbf{z}: \mathbf{z}^H \mathbf{z} = 1} [\mathbf{z}^H \mathbf{X}^H \mathbf{X} \mathbf{z}]^{1/2}$ [19, p.170]. The matrix \mathbf{I}_M stands for the $M \times M$ identity matrix and $\mathbf{0}_{M \times N}$ denotes the $M \times N$ zero matrix.

II. SIGNAL MODEL

Let $\mathbf{d}(i) = [d(iK), d(iK + 1), \dots, d(iK + K - 1)]^T$ be the i^{th} data block with length K . All elements $d(k)$, $k = iK, \dots, iK + K - 1$, are independent and identically distributed (i.i.d.). The data block $\mathbf{d}(i)$ is first multiplied

by a full-rank pre-equalization matrix $\mathbf{W} \in \mathbb{C}^{K \times K}$ and a coding matrix $\mathbf{T} \in \mathbb{C}^{N \times K}$ with $N \geq K$. Then, the signal $\mathbf{T}\mathbf{W}\mathbf{d}(i)$ is transmitted through a multi-path channel $\mathbf{h} = [h_0, h_1, \dots, h_{L-1}]^T$ with $2L-1 < K$. The i^{th} received block can be written as [7]

$$\begin{aligned} \mathbf{r}(i) &= \mathbf{R}\mathbf{H}_0\mathbf{T}\mathbf{W}\mathbf{d}(i) + \mathbf{R}\mathbf{H}_1\mathbf{T}\mathbf{W}\mathbf{d}(i-1) + \boldsymbol{\eta}(i) \\ &= \mathbf{R}(\mathbf{H}_0 + \mathbf{H}_1z^{-K})\mathbf{T}\mathbf{W}\mathbf{d}(i) + \boldsymbol{\eta}(i) \end{aligned} \quad (1)$$

in which $\mathbf{R} \in \mathbb{C}^{K \times N}$ is the receive decoding matrix, z^{-K} means a block-wise time delay, and $\boldsymbol{\eta}(i) \in \mathbb{C}^{K \times 1}$ denotes the zero-mean additive white Gaussian noise (AWGN). The convolution matrices \mathbf{H}_0 and \mathbf{H}_1 can be expressed respectively as

$$\mathbf{H}_0 = \begin{bmatrix} h_0 & 0 & 0 & \cdots & 0 \\ \vdots & h_0 & 0 & \cdots & 0 \\ h_{L-1} & \cdots & \ddots & \cdots & \vdots \\ \vdots & \ddots & \cdots & \vdots & 0 \\ 0 & \cdots & h_{L-1} & \cdots & h_0 \end{bmatrix}_{N \times N}, \quad (2)$$

and

$$\mathbf{H}_1 = \begin{bmatrix} 0 & \cdots & h_{L-1} & \cdots & h_1 \\ \vdots & \ddots & 0 & \cdots & \vdots \\ 0 & \cdots & \ddots & \cdots & h_{L-1} \\ \vdots & \ddots & \cdots & \vdots & 0 \\ 0 & \cdots & 0 & \cdots & 0 \end{bmatrix}_{N \times N}. \quad (3)$$

Equation (1) implies that the received signal for the current block is interfered by the previous block, which is known as inter-block interference (IBI). It is crucial to eliminate the IBI so as to simplify data detection. The ZP block transmission achieves this purpose [7], [8]. For the ZP scheme, the length of transmit block is set as $N = K + L - 1$ and the block coding matrix is $\mathbf{T}_{ZP} = [\mathbf{I}_K \mathbf{0}_{(L-1) \times K}^T]^T$. At the receiver, the decoding matrix is set as $\mathbf{R}_{ZP} = \mathbf{T}_{ZP}^H$. Thus, we have

$$\mathbf{R}_{ZP}\mathbf{H}_1\mathbf{T}_{ZP} = \mathbf{0}, \quad (4)$$

and

$$\mathbf{R}_{ZP}\mathbf{H}_0\mathbf{T}_{ZP} = \mathbf{H}, \quad (5)$$

in which \mathbf{H} is the $K \times K$ principal submatrix of \mathbf{H}_0 , and \mathbf{H} is a lower-triangular and banded Toeplitz matrix.

Let $\mathbf{T} = \mathbf{T}_{ZP}$ and $\mathbf{R} = \mathbf{R}_{ZP}$ in (1) and making use of (4) and (5), it yields

$$\mathbf{r}(i) = \mathbf{H}\mathbf{W}\mathbf{d}(i) + \boldsymbol{\eta}(i). \quad (6)$$

It is assumed that full CSI is known at the transmitter, which can be obtained via the principle of channel reciprocity in time-division duplex system or feedback in frequency-division duplex system. In general, the pre-equalization matrix can be designed according to ZF or MMSE criteria and they are given by [18],

$$\mathbf{W}_{ZP-ZF} = \alpha\mathbf{H}^{-1}, \quad (7)$$

and

$$\mathbf{W}_{ZP-MMSE} = \alpha\mathbf{H}^H \left[\mathbf{H}\mathbf{H}^H + \frac{1}{\rho}\mathbf{I} \right]^{-1}, \quad (8)$$

respectively, in which α is a constant used to normalize the transmit power (e.g., $\alpha = 1/||\mathbf{H}^{-1}||_F$ for ZF pre-equalizer) and ρ denotes the SNR at the receiver side.

III. STABLE INVERSE FOR NON-MINIMUM PHASE CHANNELS

In view of (7) and (8), it is obvious that ZF and MMSE pre-equalizers involve the matrix inverse operation. In the following, we illustrate the relationship between the zeros of a channel and the stability of the matrix inverse operation.

Let $h(z) = \sum_{k=0}^{L-1} h_k z^{-k}$ denote the channel \mathbf{h} in z domain and z_0, z_1, \dots, z_{L-2} be the $L-1$ zeros of $h(z)$. Its inverse system $a(z) = 1/h(z)$ is given by

$$a(z) = \sum_{k=0}^{\infty} a_k z^{-k}, \quad (9)$$

where

$$a_k = \sum_{i=0}^{L-2} b_i z_i^k, \quad (10)$$

and b_i is the residue at the pole z_i of $a(z)$. Because $a(z)$ is the deconvolution polynomial of $h(z)$ and the length of data block is K , the deconvolution matrix \mathbf{H}^{-1} can be constructed from the first K coefficients of $a(z)$. That is, \mathbf{H}^{-1} is given by

$$\mathbf{H}^{-1} = \begin{bmatrix} a_0 & 0 & 0 & \cdots & 0 \\ a_1 & a_0 & 0 & \cdots & 0 \\ \vdots & \ddots & \ddots & \cdots & \vdots \\ \vdots & \ddots & \ddots & \ddots & 0 \\ a_{K-1} & \cdots & \cdots & a_1 & a_0 \end{bmatrix}_{K \times K}. \quad (11)$$

If there exists a $|z_i| > 1$, then a_k grows exponentially with k as can be seen in (10). That is, if any zero of $h(z)$ is outside the unit circle, it leads to a poor matrix inverse. Thus, the ZF pre-equalizer in (7) works well only if $h(z)$ is of minimum phase. But this condition cannot always be satisfied in practical wireless channels. The same situation occurs for MMSE pre-equalizer in (8) when SNR is high.

In order to achieve a stable matrix inverse, a matched filter can be exploited at the transmitter to form the so-called matched zero-padded (MZP) block transmission. The following *Theorem 1* introduces how to construct the matched filter in order to guarantee the stability of the pre-equalizer in MZP transmission.

Theorem 1 (Stable Inverse Channel Construction Theorem): If a channel $h(z) = \sum_{k=0}^{L-1} h_k z^{-k}$ has no zero on the unit circle, then the inverse of $g(z) = h(z)h^*(1/z^*)$ is stable. Moreover, $g(z)$ can be decomposed into $g(z) = h_{min}(z)h_{min}^*(1/z^*)$ where $h_{min}(z)$ is of minimum phase.

Proof: Since the zeros of $g(z) = h(z)h^*(1/z^*)$ occurs in pairs: one inside the unit circle and one mirrored outside the unit circle, $g(z)$ can be decomposed into the minimum phase part $h_{min}(z)$ and its maximum phase anti-causal part $h_{min}^*(1/z^*)$ [20, Section 2.4.4]. Since both $1/h_{min}(z)$ and $1/h_{min}^*(1/z^*)$ are stable, the inverse of $g(z)$ is stable. More

specifically, $h_{min}(z)$ can be constructed by the $L - 1$ zeros z_k of $h(z)$ as

$$h_{min}(z) = \prod_{k=0}^{L-2} (z - z'_k), \quad (12)$$

where

$$z'_k = \begin{cases} z_k, & |z_k| < 1 \\ 1/z_k^*, & |z_k| > 1 \end{cases}. \quad (13)$$

An application of *Theorem 1* is that, when the matched filter $h^*(1/z^*)$ is cascaded with channel $h(z)$, the inverse of the composite channel is guaranteed to be stable. In the presence of matched filter, the received signal in (1) is modified as (see Appendix A for the derivation)

$$\mathbf{r}(i) = \mathbf{R}(\mathbf{H}_0 + \mathbf{H}_1 z^{-K}) (\mathbf{H}_0 + \mathbf{H}_1 z^{*K})^H \mathbf{T} \mathbf{W} \mathbf{d}(i) + \boldsymbol{\eta}(i). \quad (14)$$

Applying *Theorem 1* in (14) leads to

$$\begin{aligned} \mathbf{r}(i) &= \mathbf{R}(\mathbf{H}_{min,0} + \mathbf{H}_{min,1} z^{-K}) \\ &\quad \times (\mathbf{H}_{min,0} + \mathbf{H}_{min,1} z^{*K})^H \mathbf{T} \mathbf{W} \mathbf{d}(i) + \boldsymbol{\eta}(i) \\ &= \mathbf{R} \mathbf{H}_{min,0} \mathbf{H}_{min,1}^H \mathbf{T} \mathbf{W} \mathbf{d}(i+1) \\ &\quad + \mathbf{R}(\mathbf{H}_{min,0} \mathbf{H}_{min,0}^H + \mathbf{H}_{min,1} \mathbf{H}_{min,1}^H) \mathbf{T} \mathbf{W} \mathbf{d}(i) \\ &\quad + \mathbf{R} \mathbf{H}_{min,1} \mathbf{H}_{min,0}^H \mathbf{T} \mathbf{W} \mathbf{d}(i-1) + \boldsymbol{\eta}(i), \end{aligned} \quad (15)$$

where

$$\mathbf{H}_{min,0} = \begin{bmatrix} h_{min,0} & 0 & 0 & \cdots & 0 \\ \vdots & h_{min,0} & 0 & \cdots & 0 \\ h_{min,L-1} & \cdots & \ddots & \cdots & \vdots \\ \vdots & \ddots & \cdots & \ddots & 0 \\ 0 & \cdots & h_{min,L-1} & \cdots & h_{min,0} \end{bmatrix}_{N \times N} \quad (16)$$

and

$$\mathbf{H}_{min,1} = \begin{bmatrix} 0 & \cdots & h_{min,L-1} & \cdots & h_{min,1} \\ \vdots & \ddots & 0 & \cdots & \vdots \\ 0 & \cdots & \ddots & \cdots & h_{min,L-1} \\ \vdots & \ddots & \cdots & \ddots & \vdots \\ 0 & \cdots & 0 & \cdots & 0 \end{bmatrix}_{N \times N} \quad (17)$$

with $h_{min,i}$, $i = 0, \dots, L - 1$, is the i^{th} coefficient of $h_{min}(z)$ in (12).

Equation (15) implies that the received signal $\mathbf{r}(i)$ is interfered by both previous and following blocks. Fortunately, these two IBIs can be removed by zero-padded transmission strategy which forces

$$\mathbf{R}_{ZP} \mathbf{H}_{min,0} \mathbf{H}_{min,1}^H \mathbf{T}_{ZP} = \mathbf{0},$$

and

$$\mathbf{R}_{ZP} \mathbf{H}_{min,1} \mathbf{H}_{min,0}^H \mathbf{T}_{ZP} = \mathbf{0}.$$

Therefore, putting $\mathbf{T} = \mathbf{T}_{ZP}$ and $\mathbf{R} = \mathbf{R}_{ZP}$ in (15), we have

$$\begin{aligned} \mathbf{r}(i) &= \mathbf{R}_{ZP} (\mathbf{H}_{min,0} \mathbf{H}_{min,0}^H + \mathbf{H}_{min,1} \mathbf{H}_{min,1}^H) \\ &\quad \times \mathbf{T}_{ZP} \mathbf{W} \mathbf{d}(i) + \boldsymbol{\eta}(i) \end{aligned} \quad (18)$$

$$= \mathbf{G} \mathbf{W} \mathbf{d}(i) + \boldsymbol{\eta}(i), \quad (19)$$

where

$$\mathbf{G} \triangleq \mathbf{R}_{ZP} (\mathbf{H}_{min,0} \mathbf{H}_{min,0}^H + \mathbf{H}_{min,1} \mathbf{H}_{min,1}^H) \mathbf{T}_{ZP}. \quad (20)$$

It is straightforward that the ZF and MMSE pre-equalizers of (19) are,

$$\mathbf{W}_{MZIP-ZF} = \alpha \mathbf{G}^{-1}, \quad (21)$$

and

$$\mathbf{W}_{MZIP-MMSE} = \alpha \mathbf{G}^H \left[\mathbf{G} \mathbf{G}^H + \frac{1}{\rho} \mathbf{I} \right]^{-1}, \quad (22)$$

respectively, and *Theorem 1* guarantees that (21) and (22) are stable.

Remark 1: Notice that the channel state information at transmitter (CSIT) is usually perturbed due to the feedback error, its impact on the MZIP scheme is limited compared to the original pre-equalizers shown in (7) and (8). The reason is as follows. Assuming $\hat{\mathbf{G}} = \mathbf{G} + \mathbf{P}$ in which \mathbf{P} is an error matrix, we substitute $\mathbf{W}_{MZIP-ZF} = \alpha \hat{\mathbf{G}}^{-1}$ into (19) and it yields

$$\mathbf{r}(i) = \alpha (\hat{\mathbf{G}} - \mathbf{P}) \hat{\mathbf{G}}^{-1} \mathbf{d}(i) + \boldsymbol{\eta}(i) \quad (23)$$

$$= \alpha \mathbf{d}(i) - \alpha \mathbf{P} \hat{\mathbf{G}}^{-1} \mathbf{d}(i) + \boldsymbol{\eta}(i), \quad (24)$$

where the perturbed term $\mathbf{P} \hat{\mathbf{G}}^{-1}$ is bounded since $\hat{\mathbf{G}}^{-1}$ is stable when the perturbation \mathbf{P} is small enough over the non-ill-conditioned \mathbf{G} . Therefore, the effect of the CSIT error is reduced, compared to (7) and (8). Notice that in this analysis, the statistical properties of error are not taken into account. They can be exploited for a robust pre-equalizer design, but it is out of the scope of this paper.

IV. TIME-DOMAIN FAST ALGORITHMS

While computing (21) and (22), the computational complexity of a $K \times K$ matrix inverse operation is $O(K^3)$ and it sharply increases with K . The complexity can be reduced to $O(K^2)$ by exploiting the well-known Levinson-Durbin algorithm [21, p.865], but it is still high for large K . In order to further reduce the complexity, we propose a time-domain fast algorithm based on the approximate Cholesky decomposition. Before our main result is presented, we need to define the asymptotic equivalence between two matrix sequences.

Definition 1: [19, p.172] Two sequences of $k \times k$ matrices $\{\mathbf{A}_k\}$ and $\{\mathbf{B}_k\}$ are said to be asymptotically equivalent if

(1) \mathbf{A}_k and \mathbf{B}_k are uniformly bounded in strong norm:

$$\|\mathbf{A}_k\|_S, \|\mathbf{B}_k\|_S \leq M < \infty, \quad k = 1, 2, \dots$$

where M is a finite constant, and

(2) $\mathbf{A}_k - \mathbf{B}_k$ goes to zero in weak form as $k \rightarrow \infty$:

$$\lim_{k \rightarrow \infty} \|\mathbf{A}_k - \mathbf{B}_k\|_W = 0.$$

The asymptotic equivalence of the sequences $\{\mathbf{A}_k\}$ and $\{\mathbf{B}_k\}$ is abbreviated as $\mathbf{A}_k \sim \mathbf{B}_k$. It implies that \mathbf{A}_k is a close approximation to \mathbf{B}_k , and vice versa.

Then, we have the following approximate Cholesky decomposition.

Theorem 2: Let $\{\Psi_k\}$ be a sequence of finite-order positive-definite Hermitian and banded Toeplitz matrices with

the first row being $\psi = [\psi_0, \dots, \psi_{L-1}, 0, \dots, 0]_{1 \times k}$, then Ψ_k is asymptotically equivalent to

$$\Psi_k \sim \tilde{\Psi}_{min} \tilde{\Psi}_{min}^H, \quad (25)$$

where $\tilde{\Psi}_{min}$ is given by

$$\tilde{\Psi}_{min} = \begin{bmatrix} \tilde{\psi}_{min,0} & 0 & 0 & \cdots & 0 \\ \vdots & \tilde{\psi}_{min,0} & 0 & \cdots & 0 \\ \tilde{\psi}_{min,L-1} & \cdots & \ddots & \cdots & \vdots \\ \vdots & \ddots & \cdots & \ddots & 0 \\ 0 & \cdots & \tilde{\psi}_{min,L-1} & \cdots & \tilde{\psi}_{min,0} \end{bmatrix}_{k \times k} \quad (26)$$

with $\tilde{\psi}_{min,i}$, $i = 0, \dots, L-1$, are the coefficients of the minimum-phase part of $\psi(z) = \psi_0 + \sum_{i=1}^{L-1} (\psi_i z^{-i} + \psi_i^* z^i)$.

Proof: See Appendix B. ■

Applying *Theorem 2* in the MZP transmission, we have $\Psi_k = \mathbf{G}$ and $\tilde{\Psi}_{min} = \tilde{\mathbf{H}}_{min,0}$, where

$$\tilde{\mathbf{H}}_{min,0} = \mathbf{R}_{ZP} \mathbf{H}_{min,0} \mathbf{T}_{ZP}. \quad (27)$$

Then, the ZF pre-equalizer in (21) is asymptotically equivalent to [19, Theorem 1, p. 172]

$$\hat{\mathbf{W}}_{MZP-ZF} \sim \alpha \tilde{\mathbf{H}}_{min,0}^{-H} \tilde{\mathbf{H}}_{min,0}^{-1}, \quad (28)$$

whose computational complexity is $O(LK)$.

And accordingly, an asymptotically equivalent MMSE pre-equalizer with complexity $O(LK)$ is given in the following *Corollary 1*.

Corollary 1: The MMSE pre-equalizer in (22) is asymptotically equivalent to

$$\hat{\mathbf{W}}_{MZP-MMSE} \sim \alpha \mathbf{G}^H \tilde{\mathbf{G}}_{min}^{-H} \tilde{\mathbf{G}}_{min}^{-1}, \quad (29)$$

where $\tilde{\mathbf{G}}_{min} \in \mathbb{C}^{K \times K}$ is given by

$$\tilde{\mathbf{G}}_{min} = \begin{bmatrix} \tilde{g}_{min,0} & 0 & 0 & \cdots & 0 \\ \vdots & \tilde{g}_{min,0} & 0 & \cdots & 0 \\ \tilde{g}_{min,2L-2} & \cdots & \ddots & \cdots & \vdots \\ \vdots & \ddots & \cdots & \ddots & 0 \\ 0 & \cdots & \tilde{g}_{min,2L-2} & \cdots & \tilde{g}_{min,0} \end{bmatrix} \quad (30)$$

with $\tilde{g}_{min,i}$, $i = 0, \dots, 2L-2$, are the coefficients of the minimum-phase part of $g(z)g^*(1/z^*) + 1/\rho$, and $g(z) = \sum_{i=0}^{2L-2} g_i z^{-i}$ in which $[g_{2L-2}, g_{2L-3}, \dots, g_0, 0, \dots, 0]_{1 \times K}$ is the L^{th} row of \mathbf{G} .

Proof: See Appendix C. ■

Remark 2: The computational complexity of MZP-ZF in (28) and MZP-MMSE in (29) can be derived as follows. First notice that $\tilde{\mathbf{H}}_{min,0} = \mathbf{R}_{ZP} \mathbf{H}_{min,0} \mathbf{T}_{ZP}$ in (27) is of the same form as the matrix in (16) but with dimension $K \times K$. In the MZP-ZF scheme, we want to compute $\mathbf{y}(i) = \hat{\mathbf{W}}_{MZP-ZF} \mathbf{d}(i) = \alpha \tilde{\mathbf{H}}_{min,0}^{-H} \tilde{\mathbf{H}}_{min,0}^{-1} \mathbf{d}(i)$. More specifically, the calculation of $\mathbf{y}(i)$ can be divided into two consecutive steps: we first calculate $\mathbf{y}_1(i) = \tilde{\mathbf{H}}_{min,0}^{-1} \mathbf{d}(i)$ and then $\mathbf{y}(i) = \alpha \tilde{\mathbf{H}}_{min,0}^{-H} \mathbf{y}_1(i)$. As can be found in [22, Algorithm 4.3.2, p. 153], the complexity of the forward substitution is

TABLE I
ALGORITHM 1: FAST MATRIX INVERSE ALGORITHM FOR MZP-ZP
PRE-EQUALIZER

1. Calculate all $L-1$ zeros of channel $h(z)$;
2. Compute the minimum phase part $h_{min}(z)$ according to (12) and (13);
3. Construct $\tilde{\mathbf{H}}_{min,0}$ according to (16) and (27);
4. Calculate $\hat{\mathbf{W}}_{MZP-ZF} \sim \alpha \tilde{\mathbf{H}}_{min,0}^{-H} \tilde{\mathbf{H}}_{min,0}^{-1}$ in (28).

TABLE II
ALGORITHM 2: FAST MATRIX INVERSE ALGORITHM FOR MZP-MMSE
PRE-EQUALIZER

1. Calculate $g(z) = h(z)h^*(1/z^*)$;
2. Compute $\tilde{g}(z) = g(z)g^*(1/z^*) + \rho^{-1}$;
3. Find out all $4L-3$ zeros of $\tilde{g}(z)$;
4. Construct the minimum phase part $\tilde{g}_{min}(z)$ according to *Corollary 1*, and then $\tilde{\mathbf{G}}_{min}$ in (30);
5. Compute $\hat{\mathbf{W}}_{MZP-MMSE} \sim \alpha \mathbf{G}^H \tilde{\mathbf{G}}_{min}^{-H} \tilde{\mathbf{G}}_{min}^{-1}$ in (29).

$O(2LK)$. Thus, the complexity for MZP-ZF is $O(4LK)$ per transmitted vector and $O(8LK)$ for MZP-MMSE.

Remark 3: In this paper, we established a general framework to design the ZF and MMSE pre-equalizers with low computational complexity. This work includes the results in [17] as a special case, where a time-reversed filter and an approximate ZF pre-equalizer are used without stability analysis.

Summary: Combining the matched filter in Section III with the pre-equalizer in the present section, two fast matrix inverse algorithms with respect to MZP-ZF and MZP-MMSE pre-equalizers are summarized in Tables I and II, respectively.

V. SIMULATION RESULTS AND DISCUSSIONS

In this section, the Monte-Carlo simulation results are presented and some discussions follow. Simulation parameters are summarized in Table III. Simulation results are averaged over 10^5 runs. For fair comparison with different pre-equalizers, the transmit power after pre-equalizer is normalized.

We first illustrate the effect of matched filter discussed in Section III. In Fig. 1, the BER performance of ZF and MMSE pre-equalizers in ZP transmission (i.e., (7) and (8)) are compared to those in MZP transmission (i.e., (21) and (22)) when the block length $K = 64$. For compactness, the notation for a transmission scheme with a specific pre-equalizer is abbreviated. For instance, the ZP transmission with ZF pre-equalizer is abbreviated as “ZP-ZF”.

In Fig. 1, it is observed that the ZP-ZF fails to deliver a satisfactory BER performance because of the unstable channel inverse. On the contrary, the MZP-ZF outperforms the ZP-ZF because the matched filter eliminate the channel zero. For the ZP-MMSE, it achieves the best BER performance when $\text{SNR} \leq 22$ dB, since the diagonal loading term \mathbf{I}/ρ in (8) stabilize the matrix inverse at low SNR. However, it reaches a BER floor when $\text{SNR} \geq 20$ dB. For the MZP-MMSE, although it performs worse than ZP-MMSE at low SNR, it does not show any error floor and achieves lower BER when $\text{SNR} \geq 22$ dB.

Next, we compare the proposed low-complexity matrix inverse methods in (28) and (29) to the direct matrix inverse (DMI) pre-equalizers in (21) and (22) under different data

TABLE III
SIMULATION PARAMETERS

Transmit scheme	ZP, MZP
Channel length (L)	5
Prefix length	5
Block length (K)	64, 128, 256, 512, 1024
Channel coefficients distributions	i.i.d. Gaussian
Modulation type	Single-carrier QPSK

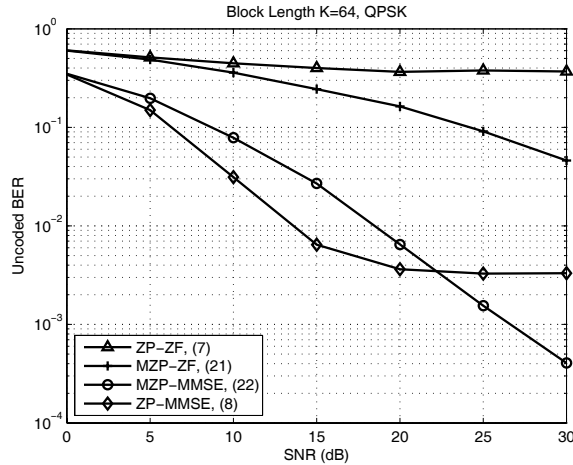


Fig. 1. BER of ZP and MZP transmission. All pre-equalizers are based on the direct matrix inverse (DMI) methods.

block lengths. In Fig. 2, the SNR is 15 dB while the block length K varies from 64 to 1024 (notice that the abscissa of Fig. 2 is in base-2 logarithmic scale). It is seen that the MZP-ZF with proposed matrix inverse method coincides well with the DMI pre-equalizer in (21). On the other hand, the MZP-MMSE with proposed matrix inverse method shows a performance difference from DMI when K is small but converges to that of DMI as K increases, and it achieves almost the same performance at $K = 1024$. Obviously, the convergence speed of the proposed MZP-MMSE in (29) is a little slower than the proposed MZP-ZF in (28). This is because the number of non-zero elements of the matrix $\tilde{\mathbf{G}}_{min}$ in (30) is twice of the matrix $\mathbf{H}_{min,0}$ in (16).

Fig. 3 compares the proposed low-complexity matrix inverse methods in (28) and (29) to the DMI pre-equalizers in (21) and (22) versus SNR, where the data block length is $K = 1024$. For MZP-ZF scheme, it is observed that the BER performance of the proposed matrix inverse method (28) is indistinguishable from the DMI method in (21) over all SNRs. However, for the MZP-MMSE scheme, the proposed matrix inverse method in (29) shows slight BER degradation with respect to the DMI method, but it still performs much better than the MZP-ZF scheme.

VI. CONCLUSIONS

Linear pre-equalizer is hard to be exploited by the zero-padded block transmission because of the possibly unstable channel inverse. In this paper, a matched zero-padded block transmission scheme is proposed to tackle the unstable channel inverse problem. Moreover, two practical ZF and MMSE

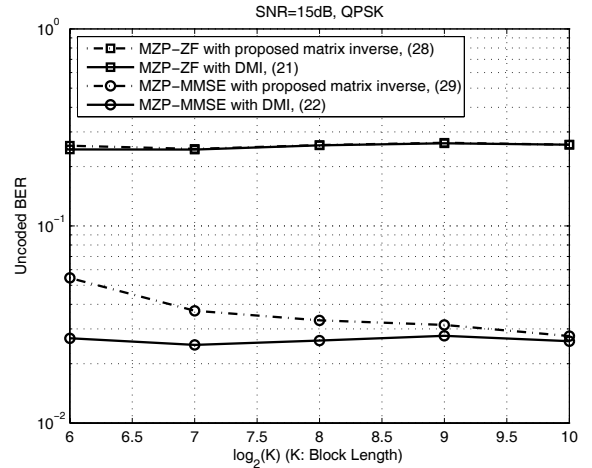


Fig. 2. BER of MZP-ZF and MZP-MMSE pre-equalizers with SNR=15dB (Proposed matrix inverse vs. DMI methods).

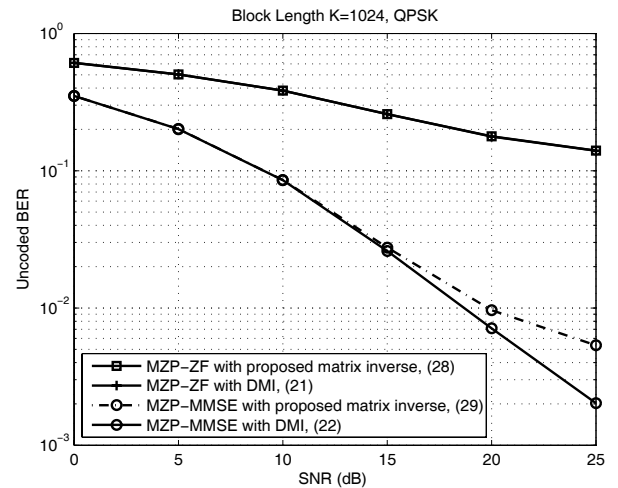


Fig. 3. BER of MZP-ZF and MZP-MMSE pre-equalizers with $K=1024$ (Proposed matrix inverse vs. DMI methods).

pre-equalizers with low computational complexity are developed by exploiting the asymptotic decomposition on banded Toeplitz matrix. They have almost the same BER performance with those based on the direct matrix inverse pre-equalizers when the data block length is large.

APPENDIX A DERIVATION OF EQ.(14)

Before the transmit signal $\mathbf{x}(i) = [x(iK), x(iK + 1), \dots, x(iK + K - 1)]^T$ is sent to the channel $h(z) = [h_0, h_1, \dots, h_{L-1}]$, a matched filter $h^*(1/z^*)$ is inserted and its output is

$$y(n) = \sum_{j=0}^{L-1} h_j^* x(n+j). \quad (31)$$

And accordingly, its block expression is given by

$$\begin{aligned} \mathbf{y}(i) &= \mathbf{H}_0^H \mathbf{x}(i) + \mathbf{H}_1^H \mathbf{x}(i+1) \\ &= (\mathbf{H}_0^H + \mathbf{H}_1^H z^K) \mathbf{x}(i) \end{aligned} \quad (32)$$

where $\mathbf{y}(i) = [y(iK), y(iK+1), \dots, y(iK+K-1)]^T$, \mathbf{H}_0 and \mathbf{H}_1 are defined in (2) and (3), respectively.

Then, $\mathbf{y}(i)$ is sent through the channel. Similar to (1), the received signal can be written as

$$\mathbf{z}(i) = (\mathbf{H}_0 + \mathbf{H}_1 z^{-K}) \mathbf{y}(i) \quad (33)$$

$$= (\mathbf{H}_0 + \mathbf{H}_1 z^{-K}) (\mathbf{H}_0 + \mathbf{H}_1 z^{*K})^H \mathbf{x}(i) \quad (34)$$

which is the signal model exploited in (14).

APPENDIX B PROOF OF THEOREM 2

Since the Hermitian Toeplitz matrix Ψ_k is positive definite, the elements of its first row $\psi = [\psi_0, \dots, \psi_{L-1}, 0, \dots, 0]_{1 \times k}$ satisfy $|\psi_0| > |\psi_i|$ for any $i \neq 0$ [20, p.765]. Furthermore, the zeros of $\psi(z) = \sum_{i=0}^{L-1} \psi_i z^{-i} + \sum_{i=-L+1}^{-1} \psi_{-i}^* z^{-i}$ occurs in pairs and therefore $\psi(z)$ can be decomposed into the minimum phase part $\tilde{\psi}_{min}(z)$ and its maximum phase anti-causal part $\tilde{\psi}_{min}^*(1/z^*)$ [20, Section 2.4.4]. That is,

$$\psi(z) = \tilde{\psi}_{min}(z) \tilde{\psi}_{min}^*(1/z^*).$$

Let $\tilde{\psi}_{min,i}$, $0 \leq i \leq L-1$, be the coefficients of $\tilde{\psi}_{min}(z)$. Similar to the derivation from (14) to (15), we have

$$\Psi_k = \tilde{\Psi}_{min} \tilde{\Psi}_{min}^H + \tilde{\Psi}_{min,1} \tilde{\Psi}_{min,1}^H, \quad (35)$$

in which $\tilde{\Psi}_{min}$ is given in (26) and

$$\tilde{\Psi}_{min,1} = \begin{bmatrix} 0 & \cdots & \tilde{\psi}_{min,L-1} & \cdots & \tilde{\psi}_{min,1} \\ \vdots & \ddots & 0 & \cdots & \vdots \\ 0 & \cdots & \ddots & \cdots & \tilde{\psi}_{min,L-1} \\ \vdots & \ddots & \cdots & \ddots & \vdots \\ 0 & \cdots & 0 & \cdots & 0 \end{bmatrix}_{k \times k}.$$

Since $\{\Psi_k\}$ and $\{\tilde{\Psi}_{min}\}$ are sequences of finite-order banded Toeplitz matrices, they are uniformly bounded in strong norm [19, Lemma 7, p.198]. Moreover, since $\tilde{\Psi}_{min,1}$ has only $L(L-1)/2$ non-zero elements, it is reasonable to assume

$$\|\tilde{\Psi}_{min,1} \tilde{\Psi}_{min,1}^H\|_F = c,$$

in which c is a real constant. Then we have

$$\begin{aligned} \lim_{k \rightarrow \infty} \|\Psi_k - \tilde{\Psi}_{min} \tilde{\Psi}_{min}^H\|_w &= \lim_{k \rightarrow \infty} \|\tilde{\Psi}_{min,1} \tilde{\Psi}_{min,1}^H\|_w \\ &= \lim_{k \rightarrow \infty} \frac{c}{\sqrt{k}} = 0. \end{aligned} \quad (36)$$

Therefore, in view of *Definition 1*, we obtain

$$\Psi_k \sim \tilde{\Psi}_{min} \tilde{\Psi}_{min}^H, \quad (37)$$

which completes the proof.

APPENDIX C PROOF OF COROLLARY 1

Although $\mathbf{G} \in \mathbb{C}^{K \times K}$ in (20) is a positive-definite Hermitian Toeplitz matrix, $\mathbf{G}\mathbf{G}^H$ is not always Toeplitz. Therefore, unlike the MZP-ZF case in (21), we cannot directly apply *Theorem 2* in the MZP-MMSE case in (22). However, notice that with $[g_{2L-2}, g_{2L-3}, \dots, g_0, 0, \dots, 0]_{1 \times K}$ being the L^{th} row of \mathbf{G} and let

$$\bar{\mathbf{G}} = \begin{bmatrix} g_{2L-2} & g_{2L-3} & \cdots & g_0 & & & \\ & g_{2L-2} & g_{2L-3} & \cdots & g_0 & & \\ & & \ddots & \ddots & \cdots & \ddots & \\ & & & g_{2L-2} & g_{2L-3} & \cdots & g_0 \end{bmatrix} \quad (38)$$

with size $K \times (K+2L-2)$,

$$\mathbf{G}_1 = \begin{bmatrix} 0 & \cdots & g_0 & \cdots & g_{L-2} \\ \vdots & \ddots & 0 & \cdots & \vdots \\ 0 & \cdots & \ddots & \cdots & g_0 \\ \vdots & \ddots & \cdots & \ddots & \vdots \\ 0 & \cdots & 0 & \cdots & 0 \end{bmatrix}_{K \times K},$$

and

$$\mathbf{G}_{-1} = \begin{bmatrix} 0 & \cdots & \cdots & \cdots & 0 \\ \vdots & \ddots & 0 & \cdots & \vdots \\ g_{2L-2} & \cdots & \ddots & \cdots & \vdots \\ \vdots & \ddots & \cdots & \ddots & \vdots \\ g_L & \cdots & g_{2L-2} & \cdots & 0 \end{bmatrix}_{K \times K},$$

we have

$$\bar{\mathbf{G}}\bar{\mathbf{G}}^H = \mathbf{G}\mathbf{G}^H + \mathbf{G}_1\mathbf{G}_1^H + \mathbf{G}_{-1}\mathbf{G}_{-1}^H. \quad (39)$$

Since $\bar{\mathbf{G}}$ is a banded Toeplitz matrix, $\bar{\mathbf{G}}$ is uniformly bounded in strong norm [19, Lemma 7, p.198], that is,

$$\|\bar{\mathbf{G}}\|_s \leq M < \infty. \quad (40)$$

Moreover, since \mathbf{G}_1 and \mathbf{G}_{-1} consist of finite number of non-zero elements, it is reasonable to assume that

$$\|\mathbf{G}_1\mathbf{G}_1^H\|_F = c_1,$$

and

$$\|\mathbf{G}_{-1}\mathbf{G}_{-1}^H\|_F = c_{-1},$$

in which c_1 and c_{-1} are real constants. Consequently, we have

$$\begin{aligned} \lim_{K \rightarrow \infty} \left\| \left(\bar{\mathbf{G}}\bar{\mathbf{G}}^H + \frac{1}{\rho} \mathbf{I} \right) - \left(\mathbf{G}\mathbf{G}^H + \frac{1}{\rho} \mathbf{I} \right) \right\|_w &= \lim_{K \rightarrow \infty} \|\mathbf{G}_1\mathbf{G}_1^H + \mathbf{G}_{-1}\mathbf{G}_{-1}^H\|_w \\ &\leq \lim_{K \rightarrow \infty} \frac{c_1 + c_{-1}}{\sqrt{K}} = 0. \end{aligned} \quad (41)$$

According to *Definition 1*, we obtain

$$\mathbf{G}\mathbf{G}^H + \frac{1}{\rho} \mathbf{I} \sim \bar{\mathbf{G}}\bar{\mathbf{G}}^H + \frac{1}{\rho} \mathbf{I}. \quad (42)$$

Recall $\bar{\mathbf{G}}$ in (38), it is straightforward that $\bar{\mathbf{G}}\bar{\mathbf{G}}^H + \frac{1}{\rho}\mathbf{I}$ is Hermitian, Toeplitz and positive definite. Therefore, according to *Theorem 2*, we have

$$\bar{\mathbf{G}}\bar{\mathbf{G}}^H + \frac{1}{\rho}\mathbf{I} \sim \tilde{\mathbf{G}}_{min}\tilde{\mathbf{G}}_{min}^H, \quad (43)$$

where $\tilde{\mathbf{G}}_{min}$ can be obtained via *Theorem 2*. Finally, combining (42) and (43) yields [19, Theorem 1, p. 172]

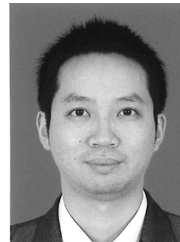
$$\mathbf{G}\mathbf{G}^H + \frac{1}{\rho}\mathbf{I} \sim \tilde{\mathbf{G}}_{min}\tilde{\mathbf{G}}_{min}^H, \quad (44)$$

which completes the proof.

REFERENCES

- [1] J. A. C. Bingham, "Multicarrier modulation for data transmission: an idea whose time has come," *IEEE Commun. Mag.*, vol. 28, no. 5, pp. 5-14, May 1990.
- [2] G. D. Forney, Jr. and M. V. Eyuboğlu, "Combined equalization and coding using precoding," *IEEE Commun. Mag.*, pp. 25-34, Dec. 1991.
- [3] A. Scaglione, G. B. Giannakis, and S. Barbarossa, "Redundant filterbank precoders and equalizers—part I: unification and optimal designs," *IEEE Trans. Signal Process.*, vol. 47, no. 7, pp. 1988-2006, July 1999.
- [4] A. Scaglione, G. B. Giannakis, and S. Barbarossa, "Redundant filterbank precoders and equalizers—part II: blind channel estimation, synchronization, and direct equalization," *IEEE Trans. Signal Process.*, vol. 47, no. 7, pp. 2007-2022, July 1999.
- [5] M. Ghogho, D. C. McLernon, E. Alameda-Hernandez, and A. Swami, "Channel estimation and symbol detection for block transmission using data-dependent superimposed training," *IEEE Signal Process. Lett.*, vol. 12, no. 3, pp. 226-229, Mar. 2005.
- [6] M. Ghogho, T. Whitworth, A. Swami, and D. McLernon, "Full-rank and rank-deficient precoding schemes for single-carrier block transmissions," *IEEE Trans. Signal Process.*, vol. 57, no. 11, pp. 4433-4442, July 2009.
- [7] Z. Wang and G. B. Giannakis, "Wireless multicarrier communications: where Fourier meets Shannon," *IEEE Signal Process. Mag.*, vol. 17, no. 3, pp. 29-48, 2000.
- [8] B. Muquet, Z. Wang, G. B. Giannakis, M. de Courville, and P. Duhamel, "Cyclic prefixing or zero padding for wireless multicarrier transmissions?" *IEEE Trans. Commun.*, vol. 50, no. 12, pp. 2136-2148, Dec. 2002.
- [9] B. Li, S. Zhou, M. Stojanovic, and L. Freitag, "Pilot-tone based ZP-OFDM demodulation for an underwater acoustic channel," in *Proc. IEEE Oceans'06*, Boston, Sep. 2006, pp. 1-5.
- [10] A. Batra, J. Balakrishnan, G. R. Aiello, J. R. Foerster, and A. Dabak, "Design of a multiband OFDM system for realistic UWB channel environments," *IEEE Trans. Microwave Theory Techniques*, vol. 52, no. 9, pp. 2123-2138, Sep. 2004.
- [11] Y. Zhou, A. I. Karsilayan, and E. Serpedin, "Sensitivity of multiband ZP-OFDM ultra-wide-band and receivers to synchronization errors," *IEEE Trans. Signal Process.*, vol. 55, no. 2, pp. 729-734, Feb. 2007.
- [12] A. Goldsmith, *Wireless Communications*. Cambridge University Press, 2005.
- [13] R. F. Fischer, *Precoding and Signal Shaping for Digital Transmission*. John Wiley & Sons Inc., 2002.
- [14] M. Tomlinson, "New automatic equalizer employing modulo arithmetic," *Electron. Lett.*, pp. 138-139, Mar. 1971.
- [15] H. Harashima and H. Miyakawa, "Matched-transmission technique for channels with intersymbol interference," *IEEE Trans. Commun.*, vol. COM-20, pp. 774-780, Aug. 1972.

- [16] R. F. H. Fischer, R. Tzschoppe, and J. B. Huber, "Signal shaping for peak-power and dynamics reduction in transmission schemes employing precoding," *IEEE Trans. Commun.*, vol. 50, pp. 736-741, May 2002.
- [17] M. R. B. Shankar and K. V. S. Hari, "Reduced complexity equalization schemes for zero padded OFDM systems," *IEEE Signal Process. Lett.*, vol. 11, no. 9, pp. 752-755, Sep. 2004.
- [18] M. Joham, W. Utschick, and J. A. Nossek, "Linear transmit processing in MIMO communications systems," *IEEE Trans. Signal Process.*, vol. 53, no. 8, pp. 2700-2712, Aug. 2005.
- [19] R. M. Gray, "Toeplitz and circulant matrices: a review," *Foundations Trends Commun. Inf. Theory*, vol. 2, no. 3, pp. 155-239, Now Publishers Inc., 2006.
- [20] D. G. Manolakis, V. K. Ingle, and S. M. Kogon, *Statistical and Adaptive Signal Processing: Spectral Estimation, Signal Modeling, Adaptive Filtering, and Array Processing*. Artech House Inc., 2005.
- [21] J. G. Proakis and D. G. Manolakis, *Digital Signal Processing: Principles, Algorithms, and Applications*, 3rd edition. Prentice Hall Press, 2004.
- [22] G. H. Golub and C. F. Van Loan, *Matrix Computations*, 3rd edition. The Johns Hopkins University Press, 1996.



Wenkun Wen received the Ph.D degree in Telecommunications Engineering from Sun Yat-sen University, Guangzhou, China, in 2007. He joined the Guangdong-Nortel R&D Center, Guangzhou, China, in 2008 as a system engineer and worked on system simulation for LTE systems. Since July 2009, He has been working with the New Postcom Equipment Co., Ltd., LTE R&D Center, Guangzhou, China, as a senior system engineer. His research interests include system performance evaluation, multi-carriers/single-carrier signal processing, space-time signal processing, and equalization for wireless communications.



Minghua Xia obtained the Ph.D. degree in Telecommunications and Information Systems from Sun Yat-sen University, Guangzhou, China, in 2007. He joined the Electronics and Telecommunications Research Institute (ETRI) of Korea, Beijing R&D Center, Beijing, China, in March 2007, where he worked as a researcher and participated in the projects on the physical layer design of 4G mobile communications. Since Aug. 2009, he has been working with the University of Hong Kong as a Postdoctoral Fellow. His research interests are in the area of network information theory, space-time signal processing, multi-user MIMO systems and cooperative relay transmission.



Yik-Chung Wu obtained the B.Eng. (EEE) degree in 1998 and the M.Phil. degree in 2001 from The University of Hong Kong (HKU). He started his Ph.D. degree in 2002 at the Texas A&M University, USA and obtained the Ph.D. degree in 2005. During his study at Texas A&M University, he was fully supported by the prestigious Croucher Foundation scholarship. From Aug. 2005 to Aug. 2006, he was with the Thomson Corporate Research, Princeton, NJ, as a Member of Technical Staff. Since Sep. 2006, he has been with the University of Hong Kong as an Assistant Professor. He was a TPC member for IEEE VTC Fall 2005, Globecom 2006, 2008, ICC 2007 and 2008. He is currently serving as an associate editor for the IEEE COMMUNICATIONS LETTERS.

Yik-Chung's research interests are in general area of signal processing and communication systems, and in particular receiver algorithm design, synchronization techniques, channel estimation and equalization.